Hierarchical Decoding Model of Upper Limb Movement Intention From EEG Signals Based on Attention State Estimation

Luzheng Bi, *Senior Member, IEEE*, Shengchao Xia, and Weijie Fei

***Abstract*— Decoding the motion intention of the human upper limb from electroencephalography (EEG) signals has important practical values. However, existing decoding models are built under the attended state while subjects perform motion tasks. In practice, people are often distracted by other tasks or environmental factors, which may impair decoding performance. To address this problem, in this paper, we propose a hierarchical decoding model of human upper limb motion intention from EEG signals based on attention state estimation. The proposed decoding model includes two components. First, the attention state detection (ASD) component estimates the attention state during the upper limb movement. Next, the motion intention recognition (MIR) component decodes the motion intention by using the decoding models built under the attended and distracted states. The experimental results show that the proposed hierarchical decoding model performs well under the attended and distracted states. This work can advance the application of human movement intention decoding and provides new insights into the study of brain-machine interfaces.**

***Index Terms*— EEG, brain-computer-interface, attention states, upper limb motion intention, hierarchical decoding model.**

I. Introduction

ELECTROENCEPHALOGRAPHY (EEG) signals can reflect brain activities [1]. Studies have shown that it is feasible to use EEG signals to decode mental states and human movement intentions [2]. As one major branch of human movement intention decoding, upper limb motion intention decoding has vital values in improving the rehabilitation and assistance of upper limb impaired patients. Researchers have conducted numerous studies on upper limb movement intention decoding from EEG signals. In 2008, Hammon *et al.* [3] were the first to extract and parse information related to hand movement from EEG signals and used this information as a feature to identify hand motion intention and direction. In 2012, Eileen *et al.* [4] used EEG signals of 0.1-4 Hz to detect the self-paced reaching movement intention of left and right hands. In 2014, López-Larraz *et al.* [5] examined motor intention from the EEG correlation of 7 different analytical upper limb movements. The percentage of correctly anticipated trials ranges from 75% to 40% (chance level of around 20%). In 2015, Jochumsen *et al.* [6] detected and classified movement-related cortical potentials (MRCPs) associated with hand movement in healthy subjects and stroke patients and showed the possibility of using the single EEG channel for detecting hand movement intention. In 2017, Muddassar *et al.* [7] used MRCPs as features and applied a matching filtering technique to detect the intention of upper limb movement and achieved a classification accuracy of 75.81%. In 2020, Yunier *et al.* [8] proposed a shoulder flexion and extension motion intention recognition system to transfer control commands to the upper limb robot exoskeleton. However, existing studies on upper limb motion intention decoding do not consider the effect of the attention state on the decoding of movement intentions. Two attention states, likely affecting the decoding performance, include alternating and divided attention. Alternating attention means that attention is shifted between dual or multiple tasks, whereas the divided attention means that attention is divided between dual or multiple tasks. In many cases, a person is in the divided attention (distracted state) during upper limb movement. The study reported in [9] showed that the intention detection accuracy might decrease when a subject is distracted, although the intention in [9] referred to the visual target detection but not human movement intention. Furthermore, by requiring subjects to perform the lower limb movement and oddball auditory tasks alternately, Aliakbaryhosseinabadi *et al.* [10] found that attention alternation decreased the magnitude of the MRCPs and reduced the detection performance of movement intentions of lower limbs. However, the studies reported in [10] do not study the effect of divided attention on the MRCPs and decoding performance of movement intention and do not propose a method to address motion intention decoding from EEG signals when a person may be in the different attention states. This paper aims to propose a hierarchical decoding model of the upper limb movement intention (movement intention means a binary classification of whether a subject intends to move), which can perform well under the attended and distracted states. The proposed decoding model includes two components. First, the attention state detection (ASD)

Manuscript received March 30, 2021; revised August 3, 2021, August 26, 2021, and September 19, 2021; accepted September 22, 2021. Date of publication September 24, 2021; date of current version October 1, 2021. This work was supported by the National Natural Science Foundation of China under Grant 51975052. *(Corresponding author: Weijie Fei.)*

This work involved human subjects or animals in its research. Approval of all ethical and experimental procedures and protocols was granted by the Local Research Ethics Committee.

The authors are with the School of Mechanical Engineering, Beijing Institute of Technology, Beijing 100081, China (e-mail: bhxblz@bit.edu.cn; shengchaoxia@163.com; 3120170241@bit.edu.cn).

Digital Object Identifier 10.1109/TNSRE.2021.3115490

component estimates the attention state during the upper limb movement. Next, the motion intention recognition (MIR) component decodes the motion intention by using the two decoding models built under the attended and distracted states, respectively. The contribution of this paper is twofold: 1) the work presented in this paper is the first to investigate the decoding of upper limb movement intention under the divided attention (distracted state); 2) this paper proposes a hierarchical decoding model of upper limb movement intention by integrating a recognition model of attention states with two decoding models of upper limb movement intention built under the attended and distracted states, respectively. This work can contribute to the research and development of human movement intention decoding robust to the distracted state and provide new insights into the study of brain-machine interfaces. The remainder of the paper is organized as follows. Section II introduces the method. Section III presents the experimental results. Section IV describes the discussion and conclusion.

II. Method

A. Participants

Twelve healthy subjects (aged 21-25, ten males and two females) participated in the experiment. All of them had normal or corrected-to-normal vision and no brain disease history. All subjects signed the informed consent forms. They were not permitted to take any alcohol, tobaccos, drugs, or caffeine before the experiment. The study adhered to the principles of the 2013 Declaration of Helsinki. Power tables from Cohen were used to evaluate the number of participants needed to obtain a significant result [11]. Given two-tailed $\alpha = 0.05$ and the recommended power level of 80%, the number of participants needed for significant results is 9, which justifies the number of subjects in our experiment.

B. Experimental Paradigm and Procedure

In this experiment, each subject was asked to complete two sub-experiments, consisting of human upper limb movements in attended and distracted states. Since all subjects were right-handed in our experiment, we regarded the right-hand movement as the upper limb movement task. In each sub-experiment, subjects were required to sit on a chair about 50 cm away from the computer screen. It was allowable to adjust the height and distance of the chair according to the comfort level of each subject. The subjects were asked to move their upper limbs rightward in a 2-D horizontal plane. Subjects were required to complete 50 trials in each sub-experiment. There was a one-minute break between the two consecutive trials and a five-minute break between the two sub-experiments. The experimental paradigms are shown in Figs. 1 and 2. The subjects were given three seconds to relax before the experiment began. At the 3rd second, a solid block appeared on the screen, representing the starting position of right hands. From this time point, subjects were in an idle state. The solid block became hollow at the 6th second, indicating that subjects prepared to move their right hands rightward.

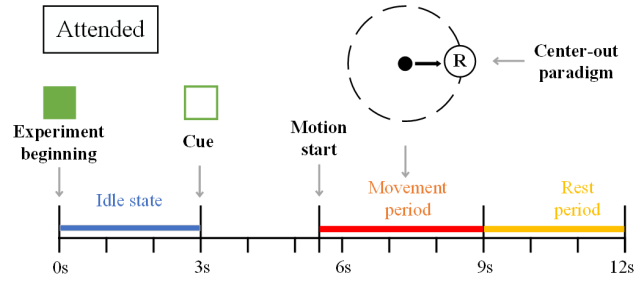

Fig. 1. Experimental paradigm of hand movement without distraction.

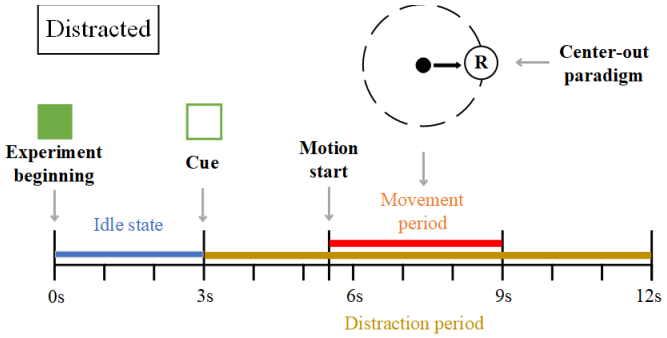

Fig. 2. Experimental paradigm of hand movement with distraction.

To avoid the visual stimulus effect, we required subjects to move their right hands in their own paces two or three seconds after the 6th second. In the sub-experiment of hand movement in the attended state, subjects were asked to move their upper limbs rightward to the designated target position. During this process, subjects were required to pay full attention to the hand movement task. In the sub-experiment of hand movement in the distracted state, we required subjects to perform the hand motion task and a cognitive task simultaneously. We used a n-back task (in this paper, $n = 2$) as the cognitive task. The n-back task has been used as a secondary task of the dual task studies [12]. The numbers were presented randomly by sound every two seconds. Participants were required to remember the most recent two numbers. Eight subjects completed the experiment according to the above procedure. However, since human brain signals are likely to be non-stationary [13]–[15], the experimental results may be purely because of the difference caused by the non-stationarity of EEG signals rather than the difference in the attention state. The issue is the well-known 'block design pitfall' pointed out by Li *et al.* in [16]. Thus, to validate whether the non-stationarity of EEG signals is a problem in our work, we designed a new experiment that randomized and interleaved the attended and distracted trials and let the remaining four subjects perform the new experiment.

C. Data Acquisition and Preprocessing

Fig. 3 shows the experimental setup. EEG signals were acquired by a 64-electrode portable wireless EEG amplifier (NeuSen. W64, Neuracle, China) from the scalp of subjects. The forehead ground was at AFz and reference was placed at CPz. The specific locations of fifty-nine channels are shown

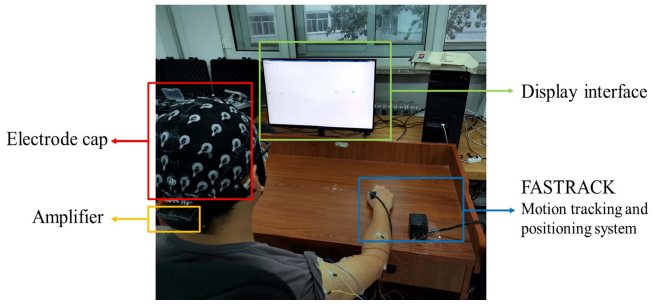

Fig. 3. Experimental setup.

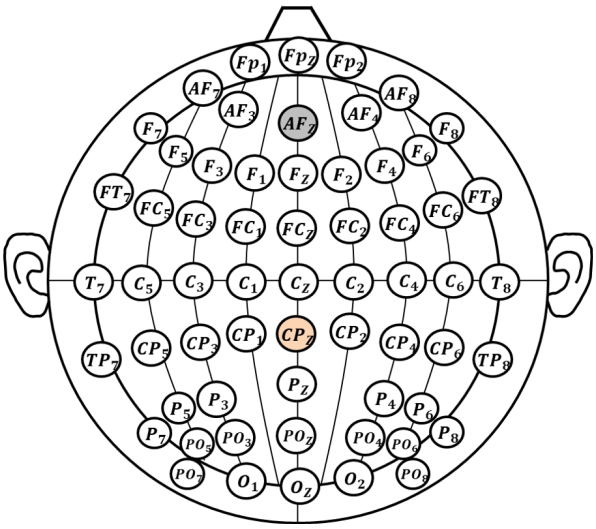

Fig. 4. EEG collection location.

in the Fig. 4. The impedance of the electrodes was kept to be less than 10 kΩ. The sampling frequency was 1000 Hz. The position of the right hand was obtained by the motion position tracking device FASTRACK at a sampling frequency of 60 Hz. We used the position information collected by FASTRACK to determine the onset of hand movement and extracted the corresponding EEG data for the analysis. When the coordinate difference between the two consecutive sampling points was greater than the threshold (preset to be 0.015 inches), it was considered the onset of hand motion. The epoch [−3, 3] s of the determined onset during each trial was selected for the subsequent analysis (0 s indicates the movement onset obtained from position analysis). We first downsampled the data to 100 Hz and used the baseline correction to remove the baseline interference signal. Then, we applied the independent component analysis (ICA) to remove ocular artifacts. Correlation coefficients of independent components (ICs) obtained from EEG signals through ICA and EOG signals were computed. The ICs with coefficients larger than 0.7 were cleared to remove the ocular artifact. The remaining ICs were inversely transformed for clean EEG data. After that, we applied artifact subspace reconstruction (ASR) to remove movement artifacts [17]. Finally, the common-average-reference (CAR) was used to filter the common interference of each channel.

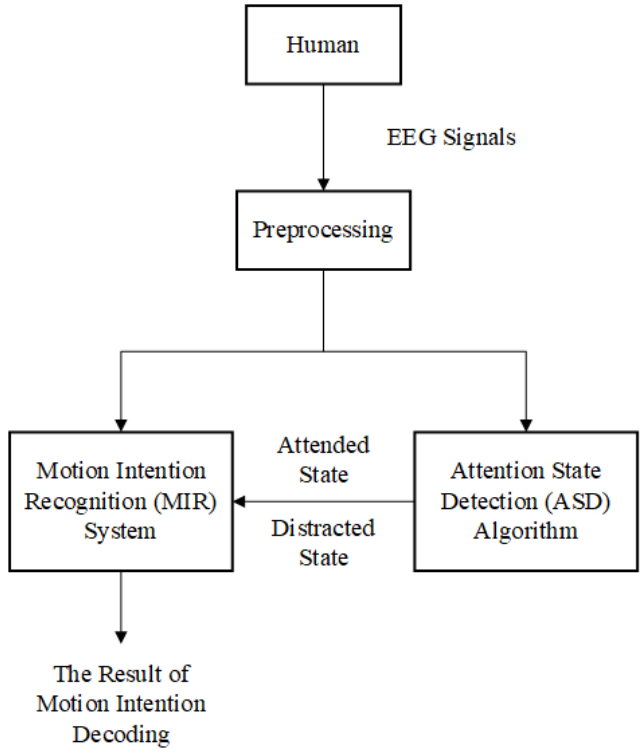

Fig. 5. Architecture of the hierarchical decoding model.

D. Hierarchical Decoding Model of Upper Limb Motion Intention

The system architecture of the proposed hierarchical decoding model, as shown in Fig. 5, consists of two major components: 1) attention state detection (ASD) and 2) motion intention recognition (MIR). The working procedure of the proposed method is as follows. The ASD component first recognizes the attention state of the subject while he/she is performing an upper limb motor task. Then, according to the attention state obtained from the ASD, the MIR system uses the corresponding motion intention decoding model to output the decoded motion intention. In this way, the whole system can decode the motion intention from EEG signals given the different attention states (including attended and distracted states).

E. ASD Algorithm

1) Preprocessing: Psychological studies have shown that attention and cognitive task are related to Alpha and Theta waves [18]–[20]. Three separable brain networks that each perform three attention functions (alerting, orienting, and executive control) involve primarily frontal and parietal brain regions [21], [22]. Fast Fourier transform (FFT) filter was used to filter EEG signals acquired from frontal and parietal brain regions in the frequency band [4], [13] Hz. The samples that we used were the window data from 1s before movement onset to the movement onset. According to the rule, one hundred and fifty samples were obtained for each subject under each attention state.

2) Feature Extraction and Classification for ASD: For each sample, we calculated the power sum of the frequency band [4], [13] Hz of EEG signals from each channel as

a classification feature. The power sums of sixteen channels (from frontal and parietal brain regions, including Fz, F1, F2, F3, F4, F5, F6, F7, F8, Pz, P3, P4, P5, P6, P7, P8) were concatenated into a sixteen-dimension feature vector. The linear discriminant analysis (LDA) was used to build a binary classifier to identify the attention state. The 5-fold cross validation was used to test the classifier. The attention state decoding models can be written as:

$$f(x) = \omega^T x + a \tag{1}$$

where $x = [x_1, x_2, \ldots, x_n]$ is the sample vector, $\omega = [\omega_1, \omega_2, \ldots, \omega_n]$ represents the projecting directions of the classifier, and a represents the threshold of the classifier, which is determined by receiver operating characteristic curve (ROC).

F. MIR Algorithm

The motion intention decoding models were established under each attention state.

1) Preprocessing: MRCP contains information that can decode the intention of the movement [23], [24]. Fast Fourier transform (FFT) filter was used to filter EEG signals in the frequency band [0.01, 4] Hz to get MRCP. The samples with no intention to move were taken from the preparation stage before the experiment, that is, 3 to 2 seconds before the start of the movement. Samples with movement intention were taken from 0.5 s before to 0.5 s after movement onset. According to the rule, one hundred and fifty samples were obtained for each subject under each attention state.

2) Feature Extraction and Classification: According to [10], [23], [25], two hundred and thirty-six temporal features (four features/channel*fifty-nine channels) were extracted from single trials of MRCP. The four features of each channel included the minimum peak negativity, the slope, the amplitude variability, and the amplitude mean. The slope was computed as the slope of the linear regression of EEG data in the time interval $[-0.5\ 0.5]$ s (0 indicates the movement onset obtained from position analysis). The amplitude variability was defined as the standard deviation of the EEG signal amplitude of each sample. The amplitude mean was defined as the average value of EEG signal amplitude of each sample. LDA was used to establish the classification model, and a 5-fold cross-validation method was used to compute the accuracy of the algorithm. The motion intention recognizing models under two attentional states can be written as:

$$\begin{cases} y_i = f_i(x) = \omega_i^T x + a_i \\ i = 1, 2 \end{cases} \tag{2}$$

where y_1 is the output of the motion intention decoding models under the attended state, and y_2 is the output of the model under the distracted state.

III. Results

A. The Effect of Distraction on Motion Intention Decoding

To validate whether the attention state can affect motion intention decoding, we first used the data obtained under the attended and distracted states in our original experiment to build the motion intention decoding model. Then, tests were performed with data in the attended and distracted states, respectively. Note that all subjects completed the 2-back task with accuracies of nearly 96%, suggesting that the primary motion task was indeed distracted. Fig.6 shows the motion intention decoding results under the attended and distracted states. We can see that the average accuracy of motion intention decoding under the attended state was 73.14%±4.86% and higher than that under the distracted state (69.86%±5.34%). Wilcoxon test showed that the accuracy difference between the two states was statistically significant ($p = 0.035 < 0.05$), which indicated that the distracted state might deteriorate the decoding performance, and we need to address this problem. Furthermore, the true positive rate (TPR) was 84.90%±12.27% under the attended state, whereas the TPR was 80.27%±15.54% under the distracted state. Wilcoxon test showed that the TPR difference between the two states was non-significant ($p = 0.225 > 0.05$). The false positive rate (FPR) was 39.55%±5.05% under the attended state, whereas FPR was 43.88%±6.87% under the distracted state. Wilcoxon test showed that the FPR difference between the two states was non-significant ($p = 0.237 > 0.05$). The Kappa Index was 0.5802±0.0569 (0.4 < Kappa Index < 0.6: moderate consistency) under the attended state, whereas Kappa Index was 0.5453 ±0.0530 (0.4 < Kappa Index < 0.6: moderate consistency) under the distracted state. Wilcoxon test showed that the Kappa Index difference between the two states was statistically significant ($p = 0.05$). These metrics also indicated that the distracted state might deteriorate the decoding performance. To test the possible confounding factor of the 'block' experimental design, we applied data from our new experiment that randomized and interleaved the attended and distracted trials to complete the same analysis. Fig. 7 shows the accuracy across four subjects. Table I shows the performance comparison between the block and interleaved designs. We found that there was performance degrading from the block design to interleaved design, suggesting the non-stationarity of EEG signals. Furthermore, we found consistent results between the original and new experiments. That is, the results of the two experiments showed that the distraction might degrade the decoding performance. For the new

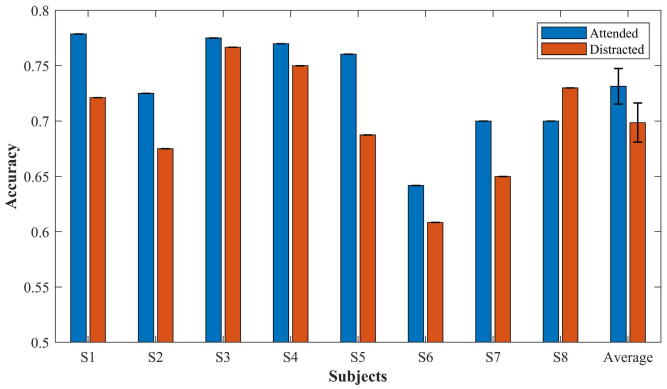

Fig. 6. The effect of distraction on movement decoding performance among S1 to S8.

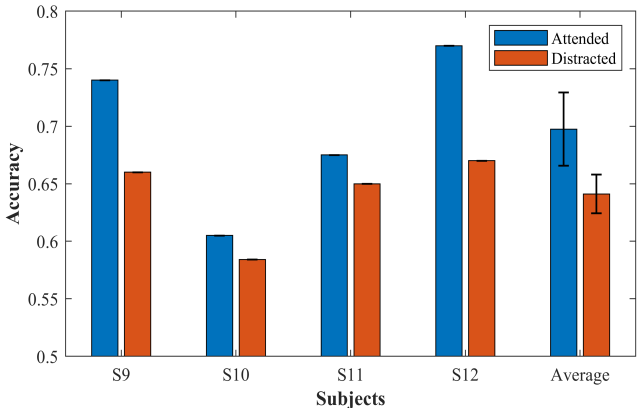

Fig. 7. The effect of distraction on movement decoding performance among S9 to S12.

TABLE I
COMPARISON OF PERFORMANCE BETWEEN BLOCK DESIGN AND INTERLEVED DESIGN

Comparison		*Acc*	*TPR*	*FPR*	*Kappa Index*
Block Design	Attended	0.7314	0.8490	0.3955	0.5802
	Distracted	0.6986	0.8027	0.4388	0.5453
Interleaved Design	Attended	0.6975	0.7913	0.4013	0.5401
	Distracted	0.6411	0.7502	0.4681	0.4735

experiment, the average accuracy of motion intention decoding under the attended state was 69.75%±7.33% and higher than that under the distracted (64.11%±3.88%). Wilcoxon test showed that the accuracy difference between the two states was marginally significant ($p = 0.05 < 0.068 < 0.1$). Furthermore, the TPR was 79.13%±22.97% under the attended state, whereas TPR was 75.02%±16.64% under the distracted state. Wilcoxon test showed that the TPR difference between the two states was non-significant ($p = 0.285 > 0.05$). The FPR was 40.13%±10.66% under the attended state, whereas FPR was 46.81%±10.43% under the distracted state. Wilcoxon test showed that the FPR difference between the two states was marginally significant ($p = 0.05 < 0.068 < 0.1$). The Kappa Index was 0.5401±0.0837 (0.4 < Kappa Index < 0.6: moderate consistency) under the attended state, whereas Kappa Index was 0.4735±0.0393 (0.4 < Kappa Index < 0.6: moderate consistency) under the distracted state. Wilcoxon test showed that the Kappa Index difference between the two states was marginally significant ($p = 0.05 < 0.068 < 0.1$).

B. Non-Stationarity Analysis of EEG Signals Between Attended and Distracted States

Since we did not consider the confounding factor (i.e., non-stationarity of EEG signals) of the 'block' experimental design in our original experiment, to further test the confounding factor, we extracted the first 3-second EEG signals (i.e., epochs) of subjects in the idle state in each trial of

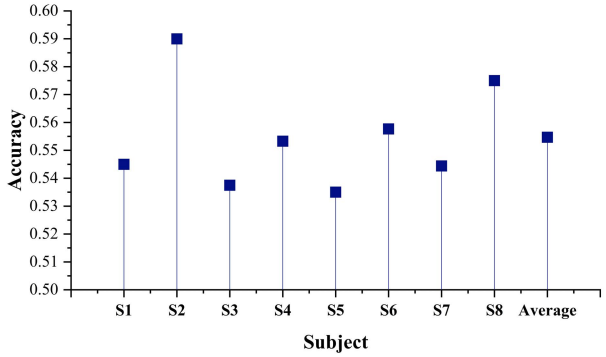

Fig. 8. Analysis results of the first 3-second of idle state.

two sub-experiments. Furthermore, we took epochs from the sub-experiment of hand movement in the attended state as one class and epochs from the sub-experiment of hand movement in the distracted state as the other class. We built a model to distinguish the two classes by using LDA with EEG magnitude as features. Experimental results from eight subjects showed the average classification accuracy of 55.47±1.19% (chance level of 50%), suggesting that the non-stationarity of EEG signals was a confounding factor in our original experiment but the effect was not significant. The detailed results are shown in Fig. 8.

C. MRCP

Figs. 9 (a), (b), and (c) show the average MRCPs of all subjects at Channels Cz, C3, and C4 in the attended and distracted states, respectively. As shown in Fig. 9, for the right-hand movements under the attended and distracted states, the negative-going trend of MRCPs appeared at around −1 s, declined rapidly after −0.5 s, and finally reached the minimum peak negativity (MPN) at around 0 s, which is the actual movement onset. The solid black line represents the average MRCP in the attended state, and the dotted red line denotes the average MRCP in the distracted state. The shadows mean the standard deviation of MRCPs over all participants. We found that the MPN at Cz under the attended state was larger than that under the distracted state (9.83 μV VS 7.17 μV), and the statistical test was significant ($p = 0.012 < 0.05$). The rebound rate (RR) at Cz, computed as the slope between the time of peak negativity (TPN) and 1 s after this point, in the attended state was larger than that in the distracted state (13.48 μV/s VS 9.56 μV/s), and the statistical test was significant ($p = 0.05$). The MPN and RR showed similar results at C3 and C4 to those at Cz. At C3, the MPN in the attended and distracted states was 8.82 μV VS 5.81 μV, and the statistical test was significant ($p = 0.012 < 0.05$). The RR in the attended and distracted states was 12.32 μV/s VS 9.23 μV/s, although the statistical test was non-significant ($p = 0.484 > 0.05$). At C4, the MPN in the attended and distracted states was 8.45 μV VS 4.92 μV, and the statistical test was significant ($p = 0.012 < 0.05$). The RR in the attended and distracted states was 11.76 μV/s VS 8.11μV/s, although the statistical test was non-significant ($p = 0.484 > 0.05$).

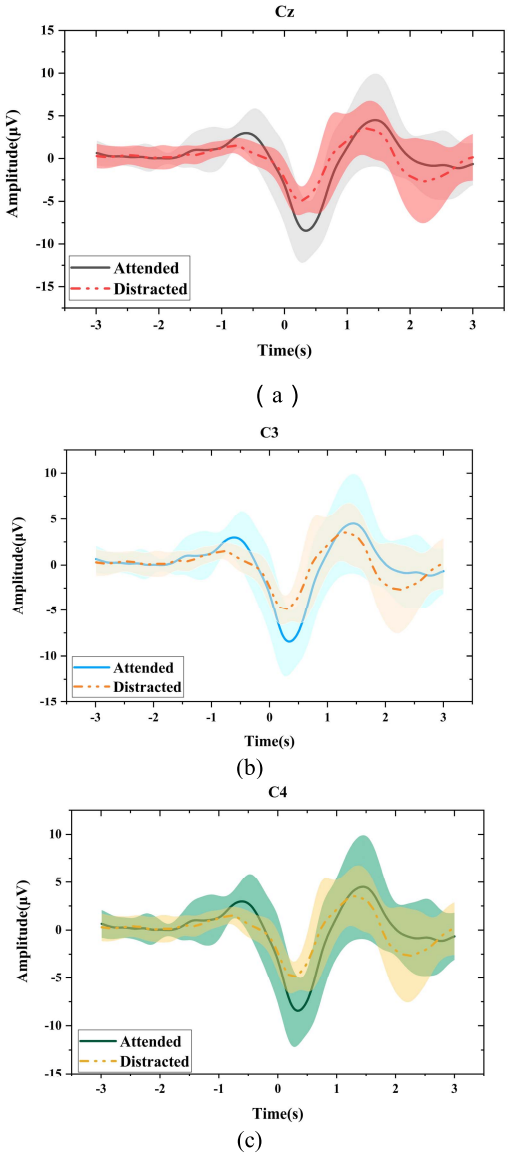

Fig. 9. MRCPs at the channels Cz, C3, and C4 under the attended and distracted states. The shadows shown in figures are the standard deviation of MRCPs over all participants. Note that 0 S means the onset of the actual movement.

D. Performance of ASD

To address the negative impact of the distracted state on decoding performance, we proposed a hierarchical decoding model. Table II shows the performance of the ASD component of the hierarchical decoding model across all subjects. We found that the average accuracy of the ASD component was 80.95%±9.90%. Furthermore, the TPR was 77.74%±11.01%. The false FPR was 17.17%±12.39%. The Kappa Index was 0.6937±0.1399 (0.6 < Kappa Index < 0.8: high consistency). These metrics showed that the ASD component performed well.

E. Performance of MIR

Table III shows the performance of the MIR component of the hierarchical decoding model across all subjects. We saw

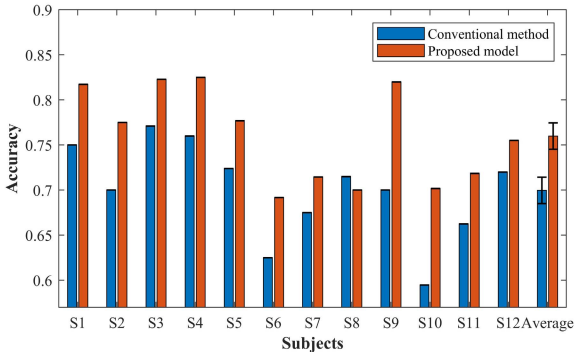

Fig. 10. Comparison of the decoding performance between the proposed model and conventional model.

that the average accuracy of the MIR component for the attended state was 78.11%±5.26%, whereas the average accuracy under the distracted state was 73.77%±5.05%. Furthermore, the TPR was 86.08%±10.21% under the attended state, whereas TPR was 82.42%±14.07% under the distracted state. The FPR was 31.86%±8.53% under the attended state, whereas FPR was 39.76%±6.62% under the distracted state. The Kappa Index was 0.6366±0.0815 (0.6 < Kappa Index < 0.8: high consistency) under the attended state, whereas Kappa Index was 0.5806±0.0691 (0.4 < Kappa Index < 0.6: moderate consistency) under the distracted state. All metrics showed the effectiveness of the MIR component under the attended and distracted states.

F. Decoding Performance of Hierarchical Decoding Model

To better show the merit of the proposed hierarchical decoding model, we compared the performance of the proposed model with that of the decoding model (hereafter we called it conventional model) built by using the conventional method reported in [10], [23], [25] based on the samples collected under the attended and distracted states. All models were tested by the five-fold cross-validation method. Fig. 10 shows the accuracy comparison results between the two models across all subjects. We saw that the proposed model outperformed the conventional model. Furthermore, the proposed model obtained an average accuracy of 75.99%±5.31%. In comparison, the average accuracy of the conventional model was 69.97%±5.32%. Wilcoxon test showed that the accuracy difference was statistically significant ($p = 0.003 < 0.05$). Furthermore, the TPR of the propose model was 87.07%±9.19%, whereas the TPR of the conventional model was 80.75%±14.82%. Wilcoxon test showed that the TPR difference was statistically significant ($p = 0.041 < 0.05$). The FPR was 36.07%±7.28% using the propose model, whereas FPR was 42.30%±6.27% using the conventional model. Wilcoxon test showed that the FPR difference was marginally significant ($p = 0.071 > 0.05$). Kappa Index was 0.6163±0.0692 (0.6 < Kappa Index < 0.8: high consistency) using the proposed model, whereas Kappa Index was 0.5441 ±0.0587 (0.4 < Kappa Index < 0.6: moderate consistency) using the conventional model. Wilcoxon test

TABLE II
PERFORMANCE OF ATTENTION STATE DETECTION ACROSS ALL SUBJECTS

Subject	S1	S2	S3	S4	S5	S6	S7	S8	S9	S10	S11	S12	*Average*	*STD*
Acc	0.9417	0.7417	0.8139	0.8533	0.9567	0.9417	0.7667	0.6500	0.7700	0.7200	0.7250	0.8333	0.8095	0.0990
TPR	0.9389	0.7333	0.7778	0.8000	0.9400	0.9389	0.7278	0.6000	0.6800	0.7000	0.7250	0.7667	0.7774	0.1101
FPR	0.0556	0.2500	0.1500	0.0933	0.0267	0.0556	0.1944	0.4600	0.1400	0.2600	0.2750	0.1000	0.1717	0.1239
Kappa Index	0.8898	0.5894	0.6862	0.7442	0.9169	0.8898	0.6216	0.5150	0.6260	0.5625	0.5686	0.7143	0.6937	0.1399

TABLE III
MOTION INTENTION DECODING PERFORMANCE UNDER ATTENDED AND DISTRACTED STATES

Subject		S1	S2	S3	S4	S5	S6	S7	S8	S9	S10	S11	S12	*Average*	*STD*
Acc	*Attended State*	0.8269	0.7750	0.8375	0.8500	0.8229	0.7000	0.7625	0.6800	0.8100	0.7700	0.7583	0.7800	0.7811	0.0526
	Distracted State	0.8077	0.7417	0.7917	0.8000	0.7500	0.6833	0.6667	0.7200	0.7900	0.6967	0.6800	0.7250	0.7377	0.0505
TPR	*Attended*	0.9231	0.9333	0.9917	0.9400	0.8750	0.6667	0.8000	0.8800	0.9400	0.7800	0.9000	0.7000	0.8608	0.1021
	Distracted	0.9231	0.8833	0.9500	0.9000	0.8542	0.6000	0.8167	0.9200	0.9200	0.8667	0.7600	0.4963	0.8242	0.1407
FPR	*Attended*	0.2692	0.3833	0.3167	0.2400	0.2292	0.2667	0.2750	0.5200	0.3200	0.2400	0.3833	0.3800	0.3186	0.0853
	Distracted	0.3077	0.4000	0.3958	0.3000	0.3542	0.4667	0.4833	0.4800	0.3400	0.4733	0.4000	0.3700	0.3976	0.0662
Kappa Index	*Attended*	0.7049	0.6327	0.7204	0.7391	0.6991	0.5385	0.5000	0.5152	0.6807	0.6260	0.6107	0.6716	0.6366	0.0815
	Distracted	0.6774	0.5895	0.6552	0.6667	0.6000	0.5190	0.5000	0.5625	0.6529	0.5354	0.5152	0.4936	0.5806	0.0691

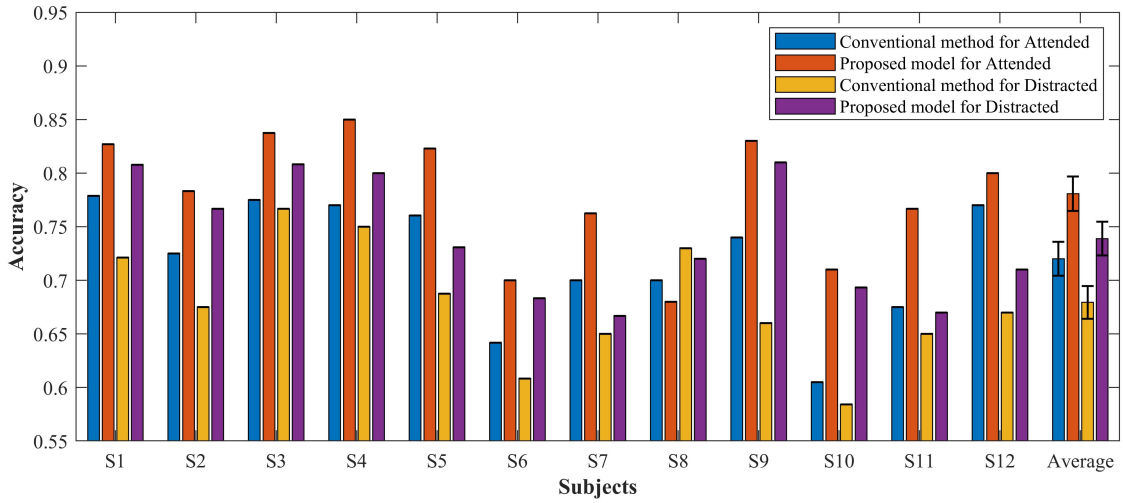

Fig. 11. Comparison of performance between the proposed model and conventional method under different concentration states.

showed that the difference in Kappa index was statistically significant ($p = 0.003 < 0.05$). Fig. 11 shows performance comparisons between the results of the proposed and convention models under two states of attention. Under the attended state, the decoding accuracy of the proposed model is 78.08%±5.79%. In comparison, the decoding accuracy of the conventional method is 72.01%±5.7%. Wilcoxon test showed that the accuracy difference was statistically significant ($p = 0.012 < 0.05$). Under the distracted state, the decoding accuracy of the proposed model is 73.89%±5.68%. In contrast, the decoding accuracy of the conventional model is 67.94%±5.5%. Wilcoxon test showed that the result difference was statistically significant ($p = 0.008 < 0.05$). The comparison results show that the proposed model has better performance in both attentional states than the conventional states.

IV. DISCUSSION AND CONCLUSION

In this paper, to address the effect of the attention state on the decoding performance of the upper limb motion intention,

we proposed a hierarchical decoding model of the upper limb motion intention by integrating a recognition model of attention states with decoding models of upper limb movement intention built under the attended and distracted states, respectively. The experimental results showed that the proposed model performed well under the attended and distracted states. This work is the first to investigate the decoding of upper limb movement intention under the distracted state. It can contribute to the research and development of human motion intention decoding (including other kinematic parameters, like velocity and position) from EEG signals. Furthermore, it can advance the application of human motion intention decoding in improving the rehabilitation and assistance of upper limb impaired patients. As shown in Fig. 9, MRCP results showed that the MPN of MRCP in the distracted state was smaller than that in the attended state. This may be due to the interference between the firing of neurons in brain regions [26]–[28] associated with movement and those associated with attention [29], [30]. According to [31], another reason might be the loss of the mental source to the upper limb motion task in the distracted state. Smaller MPN may cause lower accuracy in the detection of MRCP (i.e., the decoding of movement intention) in the distracted state. As shown in Figs. 6 and 7, the distraction impaired the motion decoding performance. To overcome the negative effect of the distraction on motion decoding, we proposed a hierarchical decoding model of the upper limb motion intention. The proposed decoding model includes two components. First, the attention state detection component estimates the attention state during the upper limb movement. Then, the motion intention recognition component decodes the motor intention by using the decoding models built under the different attention states. As shown in Fig. 10, the proposed model performed well under the attended and distracted states. Another possible method to overcome this problem is to build the decoding model (conventional model) by using the EEG data collected under both the attended and distracted states. In this paper, according to this strategy, we adopted the conventional method reported in [10], [25] to build a decoding model by using the EEG data collected under the attended and distracted states. To show the advantage of the proposed model, we compared the performance of the proposed model with that of the conventional model. As shown in Fig. 11, the proposed decoding model outperformed the conventional model across all subjects under both the attended and distracted states. Furthermore, the average accuracy of the proposed model was 6.02% higher than that of the conventional model. Our original experimental design suffers from the well-known 'block design pitfall' pointed out in [16]. That is, we did not consider one possible confounding factor (i.e., non-stationarity of human EEG signals reported in [14], [15]) of our original experimental design. Thus, the differences observed in the results may be purely because of the differences caused by the non-stationarity of EEG signals rather than the difference in the attention state. To address this problem, we added four subjects to perform a new experiment that randomized and interleaved the attended and distracted trials. The two experiments showed consistent results that the distraction might degrade the decoding performance.

This paper has some limits that need to be further handled in our future work. First, in this work, we used twelve (ten males and two females) young and healthy subjects. To further validate the findings, we need to apply more subjects, especially more old people, females, and people with disabilities. Second, although the proposed decoding model performed well, there is still a gap between the current performance and the desired one for the application. Since the hierarchical decoding model consists of the ASD and MIR components, we can improve the decoding performance by increasing the accuracies of the ASD and MIR components. For example, we can apply other kinds of features and nonlinear classifiers to improve the ASD and MIR components. Third, the motion task in this paradigm was the subjects' movement to the right. To better validate the proposed decoding model, we should consider movements in other directions. Fourth, we proposed a hierarchical decoding model to decode whether a person intends to move under the attended and distracted states. Whether the hierarchical strategy performs well for decoding other kinematic parameters under the attended and distracted states still needs to be validated. We will focus on handling these mentioned-above limitations, including adding the number of subjects, validating the findings for old people, females, and people with disabilities, further improving the decoding performance, validating the proposed model for movements in other directions, and developing other hierarchical decoding models for decoding other kinematic parameters.

ACKNOWLEDGMENT

The authors would like to thank all the subjects for volunteering to participate in their experiments.

REFERENCES

[1] B. Rohaut and L. Naccache, "Disentangling conscious from unconscious cognitive processing with event-related EEG potentials," *Rev. Neurol.*, vol. 173, nos. 7–8, pp. 521–528, Jul. 2017.

[2] O. W. Samuel, Y. Geng, X. Li, and G. Li, "Towards efficient decoding of multiple classes of motor imagery limb movements based on EEG spectral and time domain descriptors," *J. Med. Syst.*, vol. 41, no. 12, pp. 1–13, Oct. 2017.

[3] P. S. Hammon, S. Makeig, H. Poizner, E. Todorov, and V. R. de Sa, "Predicting reaching targets from human EEG," *IEEE Signal Process. Mag.*, vol. 25, no. 1, pp. 69–77, Jan. 2008.

[4] E. Lew, R. Chavarriaga, S. Silvoni, and J. R. Millan, "Detection of self-paced reaching movement intention from EEG signals," *Frontiers Neuroeng.*, vol. 5, no. 13, pp. 1–17, 2012.

[5] E. López-Larraz, L. Montesano, Á. Gil-Agudo, and J. Minguez, "Continuous decoding of movement intention of upper limb self-initiated analytic movements from pre-movement EEG correlates," *J. Neuroeng. Rehabil.*, vol. 11, no. 1, pp. 153–168, Nov. 2014.

[6] M. Jochumsen, I. K. Niazi, D. Taylor, D. Farina, and K. Dremstrup, "Detecting and classifying movement-related cortical potentials associated with hand movements in healthy subjects and stroke patients from single-electrode, single-trial EEG," *J. Neural Eng.*, vol. 12, no. 5, Aug. 2015, Art. no. 056013.

[7] M. Hussain, K. A. Bhatti, and T. Zaidi, "Muscles movement intention detection from EEG using movement related cortical potentials (MRCPs)," in *Proc. IEEE Int. Symp. Signal Process. Inf. Technol. (ISSPIT)*, Dec. 2017, pp. 366–370.

[8] Y. Prieur-Coloma *et al.*, "Enhancing shoulder pre-movements recognition through EEG Riemannian covariance matrices for a BCI-based exoskeleton," in *Proc. IEEE Int. Conf. Hum.-Mach. Syst. (ICHMS)*, Rome, Italy, Sep. 2020, pp. 1–3.

[9] M. Albares, M. Criaud, C. Wardak, S. C. T. Nguyen, S. B. Hamed, and P. Boulinguez, "Attention to baseline: Does orienting visuospatial attention really facilitate target detection?" *J. Neurophysiol.*, vol. 106, no. 2, pp. 809–816, Aug. 2011.

[10] S. Aliakbaryhosseinabadi *et al.*, "Influence of attention alternation on movement-related cortical potentials in healthy individuals and stroke patients," *Clin. Neurophysiol.*, vol. 128, no. 1, pp. 165–175, Jan. 2017.

[11] J. Cohen, *Statistical Power Analysis for the Behavioral Sciences*. Cambridge, MA, USA: Academic, 1988.

[12] S. Watter, G. M. Geffen, and L. B. Geffen, "The n-back as a dual-task: P300 morphology under divided attention," *Psychophysiology*, vol. 38, no. 6, pp. 998–1003, Nov. 2001.

[13] S. R. Liyanage, C. Guan, H. Zhang, K. K. Ang, J. Xu, and T. H. Lee, "Dynamically weighted ensemble classification for non-stationary EEG processing," *J. Neural Eng.*, vol. 10, no. 3, pp. 10–21, Apr. 2013, Art. no. 036007.

[14] P. Ahmadipour, Y. Yang, E. F. Chang, and M. M. Shanechi, "Adaptive tracking of human ECoG network dynamics," *J. Neural Eng.*, vol. 18, Aug. 2020, Art. no. 016011.

[15] H. Raza, D. Rathee, S.-M. Zhou, H. Cecotti, and G. Prasad, "Covariate shift estimation based adaptive ensemble learning for handling non-stationarity in motor imagery related EEG-based brain-computer interface," *Neurocomputing*, vol. 343, pp. 154–166, May 2019.

[16] R. Li *et al.*, "The perils and pitfalls of block design for EEG classification experiments," *IEEE Trans. Pattern Anal. Mach. Intell.*, vol. 43, no. 1, pp. 316–333, Jan. 2021.

[17] C. Chang, S. Hsu, L. Pion-Tonachini, and T. Jung, "Evaluation of artifact subspace reconstruction for automatic artifact components removal in multi-channel EEG recordings," *IEEE. Trans. Biomed. Eng.*, vol. 67, no. 4, pp. 1114–1121, Jul. 2020.

[18] J. Riddle, J. M. Scimeca, D. Cellier, S. Dhanani, and M. D. Esposito, "Causal evidence for a role of theta and alpha oscillations in the control of working memory," *Current Biol.*, vol. 30, no. 9, pp. 1748–1754. May 2020.

[19] G. G. Knyazev, "Motivation, emotion, and their inhibitory control mirrored in brain oscillations," *Neurosci. Biobehav. Rev.*, vol. 31, no. 3, pp. 377–395, Jan. 2007.

[20] L. M. Ward, "Synchronous neural oscillations and cognitive processes," *Trends Cognit. Sci.*, vol. 7, no. 12, pp. 553–559, Dec. 2003.

[21] S. E. Petersen and M. I. Posner, "The attention system of the human brain: 20 years after," *Annu. Rev. Neurosci.*, vol. 35, pp. 73–89, Jan. 2012.

[22] J. T. Coull, B. J. Sahakian, and J. R. Hodges, "The alpha (2) antagonist idazoxan remediates certain attentional and executive dysfunction in patients with dementia of frontal type," *Psychopharmacology*, vol. 123, no. 3, pp. 239–249, Feb. 1996.

[23] S. Aliakbaryhosseinabadi, E. N. Kamavuako, N. Jiang, D. Farina, and N. Mrachacz-Kersting, "Classification of EEG signals to identify variations in attention during motor task execution," *J. Neurosci. Methods*, vol. 284, pp. 27–34, Jun. 2017.

[24] D. J. Wright, P. S. Holmes, and D. Smith, "Using the movement-related cortical potential to study motor skill learning," *J. Motor Behav.*, vol. 43, no. 3, pp. 193–201, 2011.

[25] S. Aliakbaryhosseinabadi, E. N. Kamavuako, N. Jiang, D. Farina, and N. Mrachacz-Kersting, "Classification of movement preparation between attended and distracted self-paced motor tasks," *IEEE Trans. Biomed. Eng.*, vol. 66, no. 11, pp. 3060–3071, Nov. 2019.

[26] M. I. Posner, "Attention: The mechanisms of consciousness," *Proc. Nat. Acad. Sci. USA*, vol. 91, no. 16, pp. 7398–7403, Aug. 1994.

[27] J. C. Culham, P. Cavanagh, and N. G. Kanwisher, "Attention response functions: Characterizing brain areas using fMRI activation during parametric variations of attentional load," *Neuron*, vol. 32, no. 4, pp. 737–745, Nov. 2001.

[28] J. M. McDowd, "An overview of attention: Behavior and brain," *J. Neurol. Phys. Therapy*, vol. 31, no. 3, pp. 98–103, Sep. 2007.

[29] T. Hanakawa, I. Immisch, K. Toma, M. A. Dimyan, P. Van Gelderen, and M. Hallett, "Functional properties of brain areas associated with motor execution and imagery," *J. Neurophysiol.*, vol. 89, no. 2, pp. 989–1002, Feb. 2003.

[30] J. P. Gallivan, D. A. McLean, J. R. Flanagan, and J. C. Culham, "Where one hand meets the other: Limb-specific and action-dependent movement plans decoded from preparatory signals in single human frontoparietal brain areas," *J. Neurosci.*, vol. 33, no. 5, pp. 1991–2008, Jan. 2013.

[31] Y. Gu, O. F. Do Nascimento, M.-F. Lucas, and D. Farina, "Identification of task parameters from movement-related cortical potentials," *Med. Biol. Eng. Comput.*, vol. 47, no. 12, pp. 1257–1264, Sep. 2009.